

Electrical transport in bulk amorphous Se, Se-Te, Se-Sb, and Se-Te-Ge

R. M. Mehra, Radhey Shyam, and P. C. Mathur

Department of Physics and Astrophysics, University of Delhi, Delhi-110007, India

(Received 28 November 1978)

dc conductivity measurements have been made as a function of temperature and electric field in bulk amorphous Se, Se-Te, Se-Sb, and Se-Te-Ge, in order to identify the conduction mechanism and to study the effect of various dopants in Se on the conductivity. It is found that the conduction in all the samples, except in Se-Te-Ge, is through the tail of the localized states via thermally activated tunneling. In the Se-Te-Ge system, the conduction in the high-temperature region is through the extended states and in the low-temperature region via thermally activated tunneling in the localized states. It is found that the electric field effect is to increase the conductivity and to decrease the activation energy. An empirical model has been suggested to explain these results.

I. INTRODUCTION

The effect of an impurity in an amorphous semiconductor may be widely different, depending upon the conduction mechanism and the structure of the material.¹ While in crystalline semiconductors the effect of a suitable impurity is always to provide a new donor or acceptor state, this is not essential in amorphous semiconductors.² Instead of providing a localized impurity level in the forbidden gap, an impurity may merely alter the mobility of the charge carriers or may introduce structural changes³ in the amorphous material with or without modification of the localized states in the forbidden gap. Investigations of the temperature dependence of the conductivity, the effect of isoelectronic and nonisoelectronic impurities on the activation energy, and the effect of a high electric field on the conduction mechanism is a subject of great interest, because the results of such studies provide ways to control effectively the conductivity of amorphous semiconductors. The high-field effects are more readily observable in amorphous semiconductors as compared to crystalline semiconductors, because in the former, the heating effects are reasonably small due to the low mobility of the charge carriers in the localized states.

Most of the studies on the high-field conduction mechanism in the field of amorphous semiconductors have been made on thin films,⁴⁻¹⁰ and a large number of the results have been explained in terms of the Poole-Frankel effect¹¹ or in some cases by the field-aided thermal emission of carriers from the screened coulombic trap centers near the Fermi level.¹⁰ However, the conclusions drawn from such studies are not necessarily applicable to bulk materials, because the conduction properties of thin films are highly sensitive to the surface states. Moreover, the properties of thin films

markedly depend on the growing conditions, like substrate temperature during deposition, and on the method of preparation of the films. Information on the conduction phenomenon in bulk amorphous selenium (*a*-Se) is particularly lacking,¹²⁻¹⁴ in spite of the increasing possibility of using *a*-Se and its alloys in photoconduction, switching, and memory devices. Most of the work done on the study of the conduction phenomenon in *a*-Se also concerns thin films.^{4,9,15-18} Even in this case, there is quite a lot of confusion. As an example, while Rossiter and Warfield¹⁷ obtained a value of 0.0093 eV for the drift-mobility activation energy below 150 K and an increase in the activation energy by a factor of about 10 above this temperature, Tabak⁴ and Marshall *et al.*⁹ found from trap-limited drift mobility measurements an activation energy of 0.23 and 0.26 eV, respectively, below 250 K and an anomalous decrease in the activation energy at higher temperatures. Spear¹⁵ and Hartke¹⁶ have, on the other hand, found this activation energy to be 0.14 and 0.13 eV, respectively, from hole-drift-mobility measurements. Spear¹⁵ found no change in the activation energy as a function of temperature, while Hartke¹⁶ observed a small decrease above 243 K. Pfister¹⁸ found that the hole-drift-mobility activation energy in *a*-Se films is independent of temperature between 120 and 250 K and the activation energy was found to decrease slowly with electric-field increase. However, no specific temperature was found by him at which the field dependence sets in. Information on the effect of doping bulk *a*-Se and its alloys is only sparse,¹⁴⁻²⁰ although much data exist on other materials like *a*-Ge and *a*-As₂S₃.

The purpose of the present paper is to investigate the effect of Te, Sb, and Ge doping on the conductivity and activation energy of bulk *a*-Se and to study the electric-field effect on these samples in order to interpret the mechanism of

electrical conduction. The observed values of the conductivity activation energy and its dependence on the external electric field have been interpreted for the amorphous Se, Se-Te, and Se-Sb samples in terms of thermally activated tunneling in the localized states near the tail of the valence band. For the Se-Te-Ge sample, however, conduction has been found to be in the extended states in the valence band at higher temperatures and in the tail of the localized states at lower temperatures. An empirical relation has been deduced to explain the electric-field effect on the conductivity and on the activation energy.

II. EXPERIMENTAL

Various samples of Se, Se-Te, Se-Sb, and Se-Te-Ge systems of different compositions were prepared from the melt by the quenching technique which is described in our earlier paper.²⁰ The exact proportions of Se, Te, Sb, and Ge were weighed by using a microbalance. The materials were sealed in evacuated ($\sim 10^{-6}$ Torr) quartz ampoules of about 6-mm diam, in case of Se and Se-Te samples and of about 4-mm diam, in case of Se-Sb and Se-Te-Ge samples. The ampoules containing $\text{Se}_x\text{Te}_{1-x}$ were heated to about 900°C and were held at that temperature for 20–24 h, while the ampoules containing Se-Sb and Se-Te-Ge were heated to about 800°C and were held at that temperature for 24–30 h. All the ampoules were constantly agitated during heating to ensure complete mixing. The molten samples were then rapidly quenched in cold water. The quenched samples were taken out from the ampoules by dissolving the ampoules in solution of $\text{HF} + \text{H}_2\text{O}_2$ for 16–20 h. Samples of different thickness were cut with a wire cutting machine and were lapped and mirror polished. X-ray diffractometer traces of the samples were taken. Absence of sharp peaks in these traces revealed the amorphicity of the samples.

Five best samples used for the present work were having the specifications shown in Table I.

TABLE I. Specifications of the samples used in the experiment.

| Sample no. | Sample composition | Thickness (cm) | Diameter (cm) |
|------------|--|----------------|---------------|
| 1 | $\text{Se}_{90}\text{Te}_{10}$ | 0.073 | 0.6 |
| 2 | $\text{Se}_{80}\text{Te}_{20}$ | 0.093 | 0.6 |
| 3 | $\text{Se}_{70}\text{Te}_{30}$ | 0.055 | 0.6 |
| 4 | $\text{Se}_{75}\text{Sb}_{25}$ | 0.041 | 0.4 |
| 5 | $\text{Se}_{80}\text{Te}_{30}\text{Ge}_{10}$ | 0.037 | 0.4 |

Aluminum was evaporated on the entire area of the opposite faces of the samples and the electric field was applied across these faces. The samples were placed in a metallic cell (which provides proper shielding) in sandwiched configuration, and the current was measured by noting the voltage across a standard resistance with a Keithley nanovoltmeter. Observations were also taken using silver as electrode material, but no difference was observed in the experimental results due to the difference in the electrode materials. The observations were taken in the temperature range 200–300 K.

III. RESULTS AND DISCUSSION

The variation of the dc conductivity as a function of temperature ($\log \sigma$ vs $1/T$) at different electric fields for the five samples is shown in Figs. 1–5. An increase in the conductivity with the increase of electric field is observed for all the samples, which exhibit an activated temperature dependence of the form

$$\sigma = C e^{-\Delta E/kT}, \quad (1)$$

with a single activation energy ΔE , except for sample 5, which shows double activation energy.

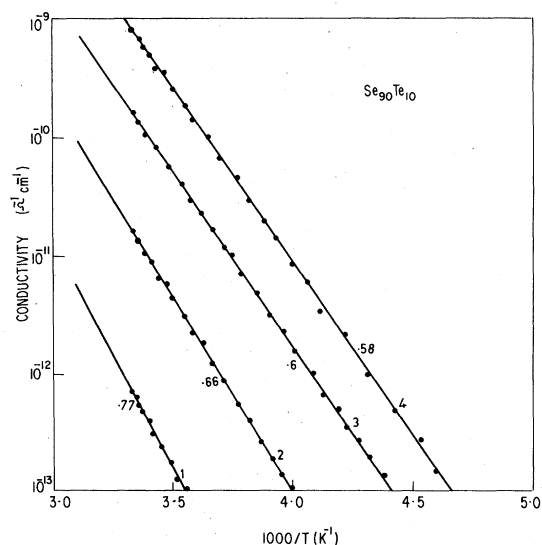


FIG. 1. Semilog plots of the conductivity vs reciprocal temperature for various values of the electric field for the $\text{Se}_{90}\text{Te}_{10}$ sample. Curves 1–4 correspond to the electric field values 4.10×10^2 , 1.37×10^3 , 2.74×10^3 , and 4.11×10^3 V/cm, respectively.

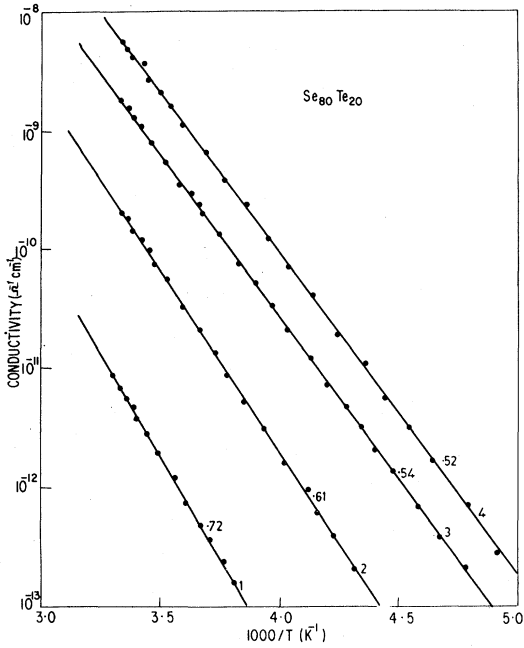


FIG. 2. Semilog plots of the conductivity vs reciprocal temperature for various values of the electric field for $\text{Se}_{80}\text{Te}_{20}$ sample. Curves 1–4 correspond to values of the electric field 3.22×10^2 , 1.07×10^3 , 2.15×10^3 , and 3.22×10^3 V/cm, respectively.

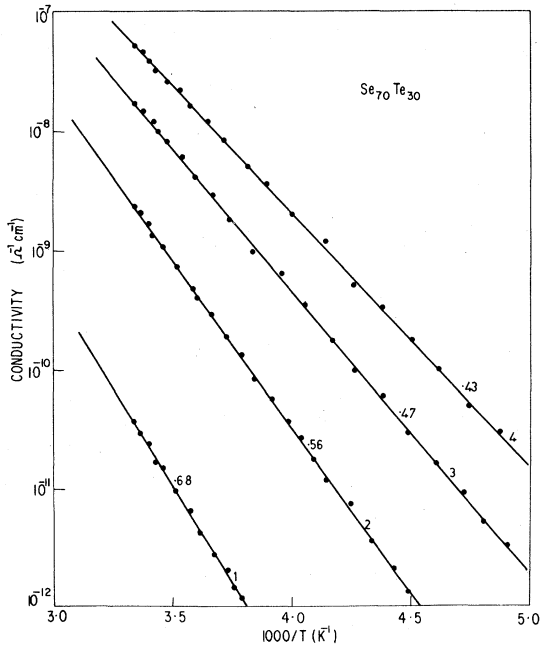


FIG. 3. Semilog plots of the conductivity vs reciprocal temperature for various values of the electric field for $\text{Se}_{70}\text{Te}_{30}$ sample. Curves 1–4 correspond to values of the electric field 5.47×10^2 , 1.82×10^3 , 3.65×10^3 , and 5.47×10^3 V/cm, respectively.

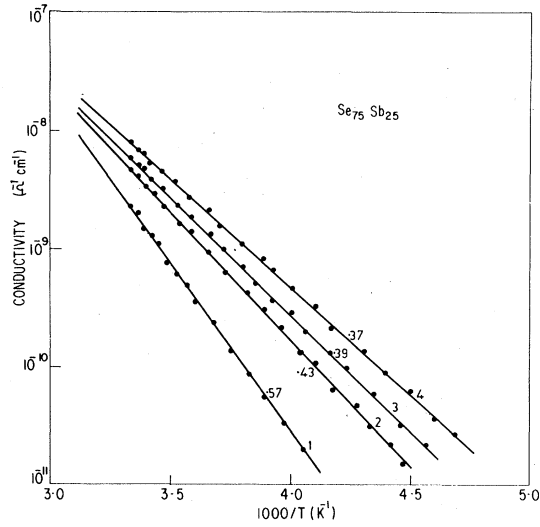


FIG. 4. Semilog plots of the conductivity vs reciprocal temperature for various values of the electric field for $\text{Se}_{75}\text{Sb}_{25}$ sample. Curves 1–4 correspond to values of the electric field 2.44×10^3 , 3.66×10^3 , 4.88×10^3 , and 6.10×10^3 V/cm, respectively.

The variation of activation energy with electric field for all the samples is shown in Fig. 6. The data for pure α -Se have been taken from our earlier work.¹⁴ It will be observed from Fig. 6, that there is a decrease in the activation energy with the increase of electric field for all the samples except for sample 5. For the $\text{Se}_x\text{Te}_{1-x}$ samples, it is also observed that this decrease becomes more predominant with the increase of Te concen-

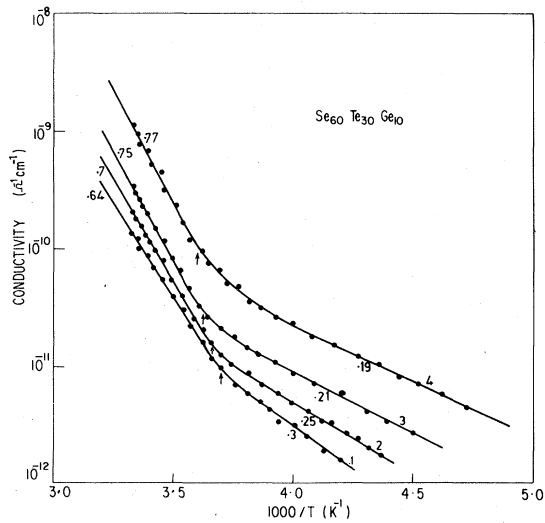


FIG. 5. Semilog plots of the conductivity vs reciprocal temperature for various values of the electric field for $\text{Se}_{60}\text{Te}_{30}\text{Ge}_{10}$ sample. Curves 1–4 correspond to values of the electric field 2.03×10^3 , 2.70×10^3 , 4.05×10^3 , and 5.40×10^3 V/cm, respectively.

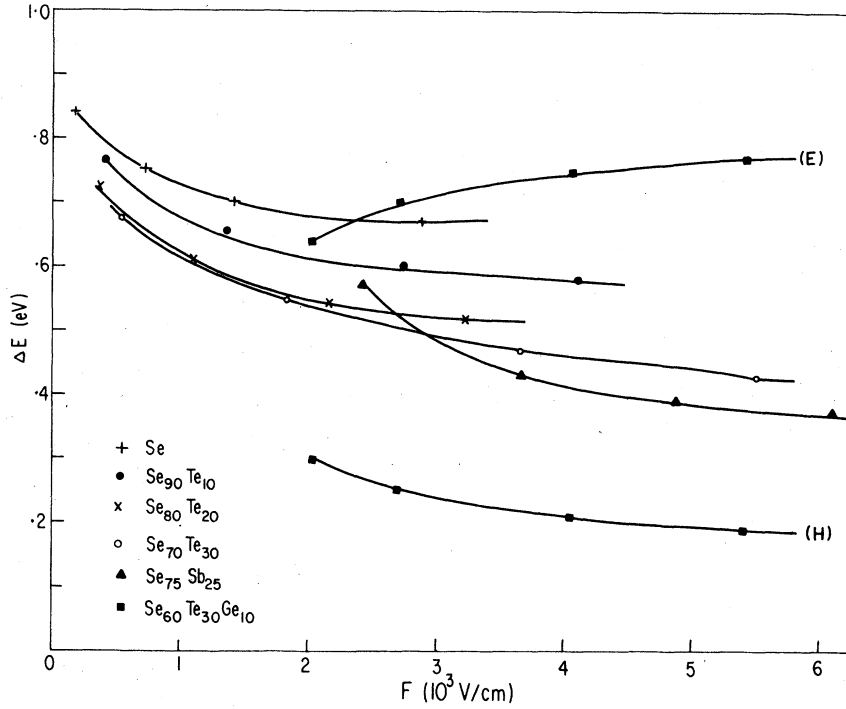


FIG. 6. Plot of activation energy vs electric field for the samples Se, $\text{Se}_{90}\text{Te}_{10}$, $\text{Se}_{80}\text{Te}_{20}$, $\text{Se}_{70}\text{Te}_{30}$, $\text{Se}_{75}\text{Sb}_{25}$, and for $\text{Se}_{60}\text{Te}_{30}\text{Ge}_{10}$ [for extended state conduction at high temperatures (E) and for hopping conduction at low temperatures (H)].

tration. It is also observed from this figure that for $\text{Se}_{60}\text{Te}_{30}\text{Ge}_{10}$ sample, the activation energy corresponding to the low-temperature region has field dependence similar to the other samples, while the high-temperature region activation energy increases with the increase of electric field. The variation of activation energy with con-

centration of Te for $\text{Se}_x\text{Te}_{1-x}$ samples is shown in Fig. 7 at different electric fields. It is found that the activation energy decreases with increase of Te concentration and this effect becomes stronger at high electric fields.

The conductivity activation energy ΔE alone does not provide any indication as to whether con-

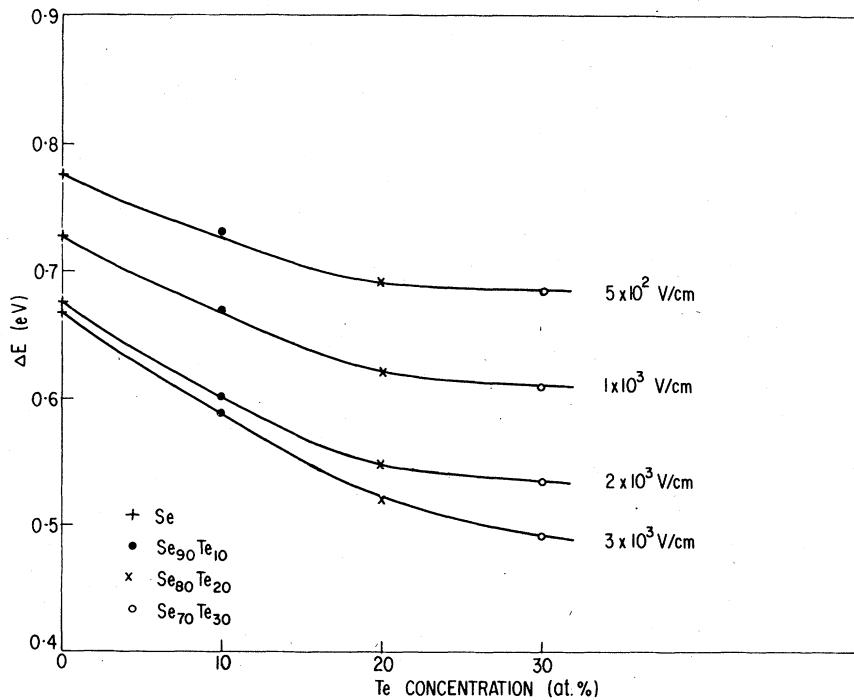


FIG. 7. Plot of activation energy vs atomic percentage of Te concentration in $\text{Se}_x\text{Te}_{1-x}$ samples at electric fields of 5×10^2 , 1×10^3 , 2×10^3 , and 3×10^3 V/cm.

TABLE II. Activation energy ΔE and preexponential factor C corresponding to the curves 1-4 (at various electric fields) and b_0 and F_0 for the samples Se, $\text{Se}_{90}\text{Te}_{10}$, $\text{Se}_{80}\text{Te}_{20}$, $\text{Se}_{70}\text{Te}_{30}$, $\text{Se}_{75}\text{Sb}_{25}$, and $\text{Se}_{80}\text{Te}_{30}\text{Ge}_{10}$.

| Sample no. | Sample composition | Curve 1 | | Curve 2 | | Curve 3 | | Curve 4 | | b_0 (eV) | F_0 (V/cm) |
|----------------|--|-----------------|-------------------------------------|-----------------|-------------------------------------|-----------------|-------------------------------------|-----------------|-------------------------------------|------------|-------------------|
| | | ΔE (eV) | C ($\Omega^{-1}\text{cm}^{-1}$) | ΔE (eV) | C ($\Omega^{-1}\text{cm}^{-1}$) | ΔE (eV) | C ($\Omega^{-1}\text{cm}^{-1}$) | ΔE (eV) | C ($\Omega^{-1}\text{cm}^{-1}$) | | |
| 0 ^a | Se | 0.84 | 4.9 | 0.75 | 2.2 | 0.70 | 2.0 | 0.67 | 1.9 | 0.56 | 1.0×10^4 |
| 1 | $\text{Se}_{90}\text{Te}_{10}$ | 0.77 | 5.3 | 0.66 | 2.4 | 0.60 | 2.1 | 0.58 | 2.0 | 0.51 | 5.0×10^3 |
| 2 | $\text{Se}_{80}\text{Te}_{20}$ | 0.72 | 7.5 | 0.61 | 4.0 | 0.54 | 2.3 | 0.52 | 2.2 | 0.46 | 5.6×10^3 |
| 3 | $\text{Se}_{70}\text{Te}_{30}$ | 0.68 | 15.9 | 0.56 | 6.3 | 0.47 | 2.4 | 0.43 | 2.3 | 0.42 | 5.8×10^3 |
| 4 | $\text{Se}_{75}\text{Sb}_{25}$ | 0.57 | 2.5 | 0.43 | 7.9×10^{-2} | 0.39 | 2.0×10^{-2} | 0.37 | 1.4×10^{-2} | 0.35 | 6.5×10^3 |
| 5 | $\text{Se}_{80}\text{Te}_{30}\text{Ge}_{10}$ (H) | 0.30 | 3.1×10^{-6} | 0.25 | 5×10^{-7} | 0.21 | 1.4×10^{-7} | 0.19 | 1.3×10^{-7} | 0.18 | 5.7×10^3 |
| | $\text{Se}_{80}\text{Te}_{30}\text{Ge}_{10}$ (E) | 0.64 | 7.9 | 0.70 | 1.2×10^2 | 0.75 | 1.4×10^3 | 0.77 | 9.5×10^3 | | |

^a Reference 14.

duction takes place in extended states above the mobility edge or by hopping in the localized states. The activation energy, in the former case, represents the difference of energy between the mobility edge and the Fermi level. In the latter case, the activation energy represents the sum of the energy separation between the occupied localized states and the Fermi level and the mobility activation energy for the hopping process between the localized states. It was suggested by Mott²¹ that the preexponential factor C of Eq. (1) for conduction in the localized states is about two to three orders smaller than for conduction in the extended states. The values of C , obtained from the intercepts of $\log \sigma$ vs $1/T$ plots for all the samples, are shown in Table II. It is clear from Table II, that in case of the $\text{Se}_{60}\text{Te}_{30}\text{Ge}_{10}$ sample, the numerical values of C and ΔE for the high-temperature region, in comparison to the corresponding values for the low-temperature region, indicate, that the transport of carriers in the high-temperature region is through the extended states and in the low-temperature region, the conduction is by hopping in the localized states. It may be mentioned, that in practice, both of these conduction mechanisms may occur simultaneously, with the localized states conduction gradually becoming predominant at lower temperatures. This is due to the fact that with decreasing temperature, the probability of thermal release of the carriers from the localized states near the mobility edge becomes rapidly smaller and a charge carrier is more likely to hop to a neighboring site in the distribution. In the Se and $\text{Se}_x\text{Te}_{1-x}$ samples, the conduction process, in the entire temperature region of observation, is via hopping in the localized states because the observed values of the activation energy, shown in Table II, are less than the reported values of the half of the mobility gaps of amorphous Se and Se-Te systems.²² More important than this, the observed values of C are $\sim 10 \Omega^{-1}\text{cm}^{-1}$ for all the samples, while for the conduction in the extended states, the reported²² value of C for α -Se and α -Se-Te systems are $\sim 10^4 \Omega^{-1}\text{cm}^{-1}$. The observations of the extended state conduction in the $\text{Se}_{60}\text{Te}_{30}\text{Ge}_{10}$ sample, implies, that the addition of Ge increases the probability of release of the carriers from the localized states due to the thermal excitation. It has been observed²³ that the addition of Ge weakens the structure due to increase in weaker Ge-Ge bonds and this weakening of the bonds can be a probable reason for the double activation energy observed in the $\text{Se}_{60}\text{Te}_{30}\text{Ge}_{10}$ sample.

As seen from Table II, the addition of Sb in Se, lowers appreciably the activation energy, which implies that either there is a large decrease in

the optical band gap of Se-Sb system or the width of the localized state region increases or both.

The increase in the value of C due to addition of Te is attributed to the increase in the density of localized states with the increase of Te, which is the main reason for such a large increase in the conductivity as has been observed in the Te doped samples. A decrease in the optical gap of Se has also been found by the addition of Te.²⁴ Since the electrical gap of a -Te is very much smaller than that of a -Se, the decrease of ΔE and hence increase of conductivity with Te concentration is expected. This could also be the cause of the further lowering of the activation energy on addition of Ge of the $\text{Se}_{60}\text{Te}_{30}\text{Ge}_{10}$ sample in the hopping conduction region, as observed in the present experiment.

The increase of conductivity due to electric field is attributed generally to the following effects: (i) the emission of carriers from coulombic centers because of the lowering of barriers with the application of electric field (i.e., Poole Frenkel or Poole effect¹¹); (ii) contact induced effect (space charge limited current); (iii) thermal effect due to Joule heating of the sample.

Since the observed data could not be fitted either with $\log \sigma$ vs $E^{1/2}$ or $\log \sigma$ vs E plot over the entire range of the applied electric field, the Poole Frenkel and Poole effect can not be considered in the present case. The independence of conductivity on the electrode materials rules out the possibility of space charge limited current. As the resistance of the sample is very high, the increase of conductivity due to Joule heating of the sample can also be discarded.

The value of preexponential factor C for all the samples, is found to decrease with electric field

as shown in Table II. Since the trap-limited mobility increases²⁵ only slightly with field or remains constant,²⁶ it implies that there is a decrease in the density of localized states with the increase of electric field. This is possible if the carriers drift in the higher localized states with the increase of electric field besides being thermally agitated in the tail of the localized states.

The observed decrease of the activation energy with electric field can therefore be explained by assuming the drift of the carriers in the localized states, besides the normal conduction process due to thermally activated tunneling in the tail of the localized states. For the $\text{Se}_{60}\text{Te}_{30}\text{Ge}_{10}$ sample, the increase of the activation energy with electric field in the extended state region (at high temperatures) can be understood by assuming that the contribution to the conductivity activation process is due to conduction in the extended states and also due to hopping in the localized states. With the increasing electric field, as the former process, which is having a high activation energy, becomes more predominant due to the dumping of the carriers in the extended states, the effective activation energy of the system increases, inspite of the fact that the activation energy of the extended state conduction may remain constant.²⁷ The observed results for the hopping conduction can be explained by expressing the field dependence of the conductivity by the relation

$$\sigma = C \exp\{-[\Delta E - b(F)]/kT\}, \quad (2)$$

where $b(F)$ is an increasing function of the field which should saturate at high fields so as to make the total activation energy for the conduction process equal to ΔE_v , the trap depth. A possible functional form of $b(F)$ describing the above men-

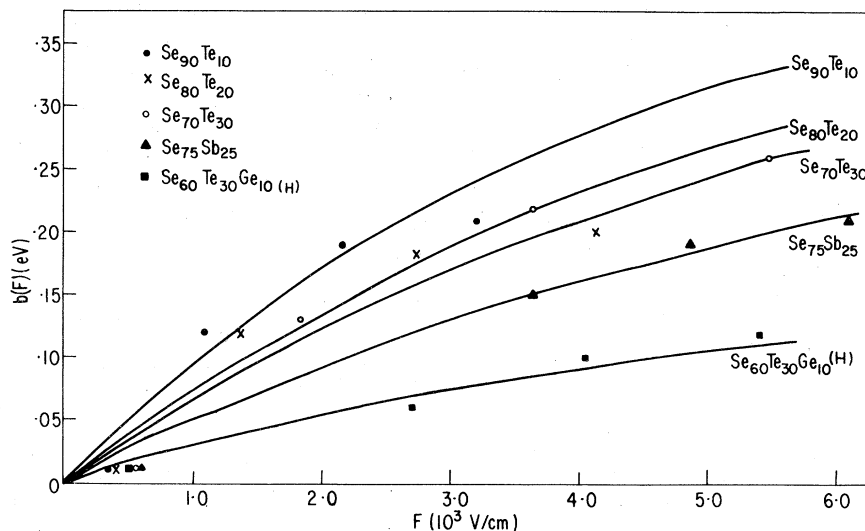


FIG. 8. Plot of $b(F)$ vs electric field for the samples $\text{Se}_{90}\text{Te}_{10}$, $\text{Se}_{80}\text{Te}_{20}$, $\text{Se}_{70}\text{Te}_{30}$, $\text{Se}_{75}\text{Sb}_{25}$, and $\text{Se}_{60}\text{Te}_{30}\text{Ge}_{10}$ (H). Continuous curves are the plots of Eq. (3) for all the samples.

tioned feature is

$$b(F) = b_0[1 - \exp(-F/F_0)], \quad (3)$$

where b_0 is the saturated value of $b(F)$ and F is the applied field. The variation of $b(F)$ with F is shown in Fig. 8. The values of b_0 and F_0 , with which our data fit, are given in Table II.

The physical significance of $b(F)$ in this model is that this parameter represents the contribution of conduction due to drifting process of the charge carriers in the localized states. The value of $b(F)$ increases with the field, which means that with increasing field, the carriers occupy higher-energy states in the localized states region and the contribution of the drift process to the conductivity increases, resulting in a lowering of the activation energy with the increase of electric field. Since the addition of Te lowers the activation energy of the thermally activated hopping process, the relative contribution of this process increases as compared to the field induced drift process,

thereby reducing the value of $b(F)$ with the increase of Te concentration. The saturated values of $b(F)$, i.e., b_0 should also decrease with the increase of Te concentration due to the same reason, which is an experimentally observed fact.

It may be mentioned that Shklovskii²⁸ found that the electric field dependence of heavily doped, highly compensated Ge crystals can be described by the relation,

$$\sigma(E) \sim \exp(E_0/E)^{1/4}, \quad (4)$$

in the field region >1 kV/cm, while for lower fields, the conductivity in these samples was found to obey the relation,

$$\sigma(E) = \sigma(0) \exp(eER/T), \quad (5)$$

which is a theoretical relation derived by Hill,²⁹ R being the average distance of hopping. We have, however, not observed linear relationship between $\log\sigma(E)$ and E .

¹N. F. Mott, *Philos. Mag.* **19**, 835 (1969).

²G. B. Abdullaev, S. I. Mekhtieva, D. S. Abidinov, and G. M. Aliev, *Phys. Status Solidi* **11**, 891 (1965).

³V. A. Twaddell, W. C. Lacourse, and J. D. Mackenzie, *J. Non-Cryst. Solids* **8-10**, 831 (1972).

⁴M. D. Tabak, *Phys. Rev. B* **2**, 2104 (1970).

⁵N. Croitoru and L. Vescan, *Thin Solid Films* **3**, 269 (1969).

⁶M. Morgan and P. A. Walley, *Philos. Mag.* **23**, 661 (1971).

⁷A. H. Clark and T. J. Burke, *Phys. Rev. Lett.* **28**, 678 (1972).

⁸D. L. Camphansen, G. A. N. Cornell, and W. Paul, *J. Non-Cryst. Solids* **8-10**, 223 (1972).

⁹J. M. Marshall, C. Main, and A. E. Owen, *J. Non-Cryst. Solids* **8-10**, 760 (1972).

¹⁰T. Suzuki, M. Hirose, and Y. Osaka, *J. Non-Cryst. Solids* **23**, 1 (1977).

¹¹J. Frenkel, *Phys. Rev.* **54**, 647 (1938).

¹²G. Juska, A. Mataliones, A. Sakalas, and J. Viscakas, *Phys. Status Solidi K* **36**, 121 (1969).

¹³A. I. Lakatos and M. Abkowitz, *Phys. Rev. B* **3**, 1791 (1971).

¹⁴R. M. Mehra, P. C. Mathur, A. K. Kathuria, and

Radhey Shyam, *J. Phys. Chem. Solids* **39**, 295 (1978).

¹⁵W. E. Spear, *Proc. Phys. Soc. Lond. B* **76**, 826 (1960).

¹⁶J. L. Hartke, *Phys. Rev.* **125**, 1177 (1962).

¹⁷E. L. Rossiter and G. Warfield, *J. Appl. Phys.* **42**, 2527 (1971).

¹⁸G. Pfister, *Phys. Rev. Lett.* **36**, 271 (1976).

¹⁹J. Schottmiller, M. Tabak, G. Lucovsky, and A. Ward, *J. Non-Cryst. Solids* **4**, 80 (1970).

²⁰R. M. Mehra, P. C. Mathur, A. K. Kathuria, and Radhey Shyam, *Phys. Rev. B* **18**, 5620 (1978).

²¹N. F. Mott, *Philos. Mag.* **22**, 7 (1970).

²²E. A. Davis and N. F. Mott, *Philos. Mag.* **22**, 903 (1970).

²³J. de Neufville, *J. Non-Cryst. Solids* **8-10**, 85 (1972).

²⁴H. P. D. Lanyon, *J. Appl. Phys.* **35**, 1516 (1964).

²⁵J. M. Marshall and A. E. Owen, *Philos. Mag.* **24**, 1281 (1971).

²⁶P. G. Le Comber and W. E. Spear, *Phys. Rev. Lett.* **25**, 509 (1970).

²⁷N. F. Mott, *Philos. Mag.* **24**, 911 (1971).

²⁸B. I. Shklovskii and A. L. Efros, *J. Exp. Theor. Phys.* **62**, 1156 (1972).

²⁹R. M. Hill, *Philos. Mag.* **24**, 1307 (1971).